Pinnatins A−E: Marine Diterpenes of the Rare Gersolane Class Derived from a Photochemically Induced Rearrangement of a Conjugated 2,5-Bridged Furanocembrane Precursor

Abimael D. Rodríguez,* Jian-Gong Shi, and Songping D. Huang

Department of Chemistry, University of Puerto Rico, P.O. Box 23346, Río Piedras, Puerto Rico 00931-3346, and Center for Molecular and Behavioral Neuroscience, Universidad Central del Caribe, Bayamón, Puerto Rico 00960-3001

Received February 11, 1998

A group of five highly functionalized polycyclic α,γ-disubstituted-α,β-unsaturated-γ-lactones (**3**−**7**) featuring a unique bicyclo [11.1.0] carbon skeleton joined in a trans fashion have been isolated from a Caribbean gorgonian, *Pseudopterogorgia bipinnata*. These rare marine diterpenoids can be regarded as representatives of the uncommon gersolane ring system. Two of the new metabolites, pinnatin A (**3**) and pinnatin B (**4**), showed significant differential antitumor activity in the National Cancer Institute's 60-cell-line tumor panel. The biogenesis of the pivotal metabolite pinnatin A (**3**) appears to involve a photochemically allowed [$_o2_a + {}_\pi2_a$] cycloaddition process of a conjugated 2,5-bridged furanocembrane precursor. Structural assignments were accomplished through extensive spectroscopic analysis including 2D NMR, accurate mass measurements (HREIMS), X-ray crystallography, and chemical interconversions.

Introduction

Caribbean gorgonian octocorals continue to be a rich source of secondary metabolites with novel structures and desirable biological activity.[1,2] In a continuing search for potential chemotherapeutic agents from marine organisms, we have isolated a family of five diterpenoid lactones from the Caribbean sea plume *Pseudopterogorgia bipinnata* (Gorgonacea) (Verrill).[3] These cancer cell cytotoxins, trivially named pinnatins, are highly functionalized polycyclic α,γ-disubstituted-α,β-unsaturated-γ-lactones, and their structures, which feature a unique bicyclo [11.1.0] carbon skeleton joined in a trans fashion, were determined by detailed spectroscopic analysis and confirmed by single-crystal X-ray diffraction experiments (Figure 1). The pinnatins are minor secondary metabolites which can be regarded as examples of diterpenoids of the uncommon gersolane ring system. Thus far, only one gersolane-type diterpene has been reported in the literature. This minor metabolite, named gersolide, was isolated in 1987 from the Atlantic Ocean soft coral *Gersemia rubiformis* (Alcyonaria) by the Andersen and Clardy groups.[4] Unfortunately, the paucity of material precluded their attempts to describe the spectroscopic details of gersolide.[5] In that report Andersen and Clardy theorized that since *G. rubiformis* contained similarly functionalized diterpenoids having cembrane, pseudopterane, and gersolane skeletons, it seemed plausible that the latter two skeletons arise from rearrangements of a cembrane precursor. This theory drew upon that advanced earlier by Fenical et al. who had speculated that pseudopteranes might arise from a ring contraction of a cembranoid precursor rather than through a process involving dimerization of two geranyl units.[6] No confirming data, however, were provided by either group of authors to support these hypotheses. In a recent communication, we demonstrated for the first time the biogenetic relationship between two diterpenoids of the cembrane and pseudopterane classes.[7] We found that upon irradiation in acetonitrile solution the furanocembranolide bipinnatin J (**1**) affords directly the known pseudopterane kallolide A (**2**).[7,8] This facile cycloisomerization reaction appears to involve a photochemical suprafacial [1,3]-sigmatropic rearrangement with retention of configuration at the migrating α,β-unsaturated-γ-butenolide group (Figure 2). In addition to describing for the first time the structures and the complete chemical and spectroscopic properties of five new gersolane diterpenes, we also report confirming evidence which

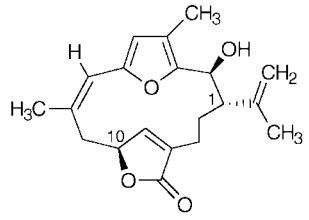

Bipinnatin J (1)

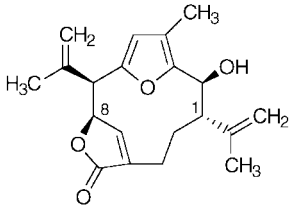

Kallolide A (2)

† Phone: (787)-764-0000, ext 4799. Fax: (787)-751-0625. E-Mail: arodrig@goliath.cnnet.clu.edu.

(1) Faulkner, D. J. *Nat. Prod. Rep.* **1997**, *14*, 259−302 and previous papers in this series.

(2) Rodríguez, A. D. *Tetrahedron* **1995**, *51*, 4571−4618.

(3) For previous studies related to *P. bipinnata*, see: (a) Fenical, W. *J. Nat. Prod.* **1987**, *50*, 1001−1008. (b) Wright, A. E.; Burres, N. S.; Schulte, G. K. *Tetrahedron Lett.* **1989**, *30*, 3491−3494. (c) Culver, P.; Burch, M.; Potenza, C.; Wasserman, L.; Fenical, W.; Taylor, P. *Mol. Pharmacol.* **1985**, *28*, 436−444. (d) Abramson, S. N.; Trischman, J. A.; Tapiolas, D. M.; Harold, E. E.; Fenical, W.; Taylor, P. *J. Med. Chem.* **1991**, *34*, 1798−1804.

(4) Williams, D. E.; Andersen, R. J.; Parkanyi, L.; Clardy, J. *Tetrahedron Lett.* **1987**, *28*, 5079−5080.

(5) The structure of gersolide was solved by a single-crystal X-ray diffraction analysis. Only partial ^{1}H NMR data and the *m/z* value for the parent ion of gersolide were reported.

(6) Bandurraga, M. M.; Fenical, W.; Donovan, S. F.; Clardy, J. *J. Am. Chem. Soc.* **1982**, *104*, 6463−6465.

(7) Rodríguez, A. D.; Shi, J.-G. *J. Org. Chem.* **1998**, *63*, 420−421.

(8) Look, S. A.; Burch, M. T.; Fenical, W.; Qi-tai, Z.; Clardy, J. *J. Org. Chem.* **1985**, *50*, 5741−5746.

S0022-3263(98)00256-4 CCC: $15.00
Published on Web 05/30/1998

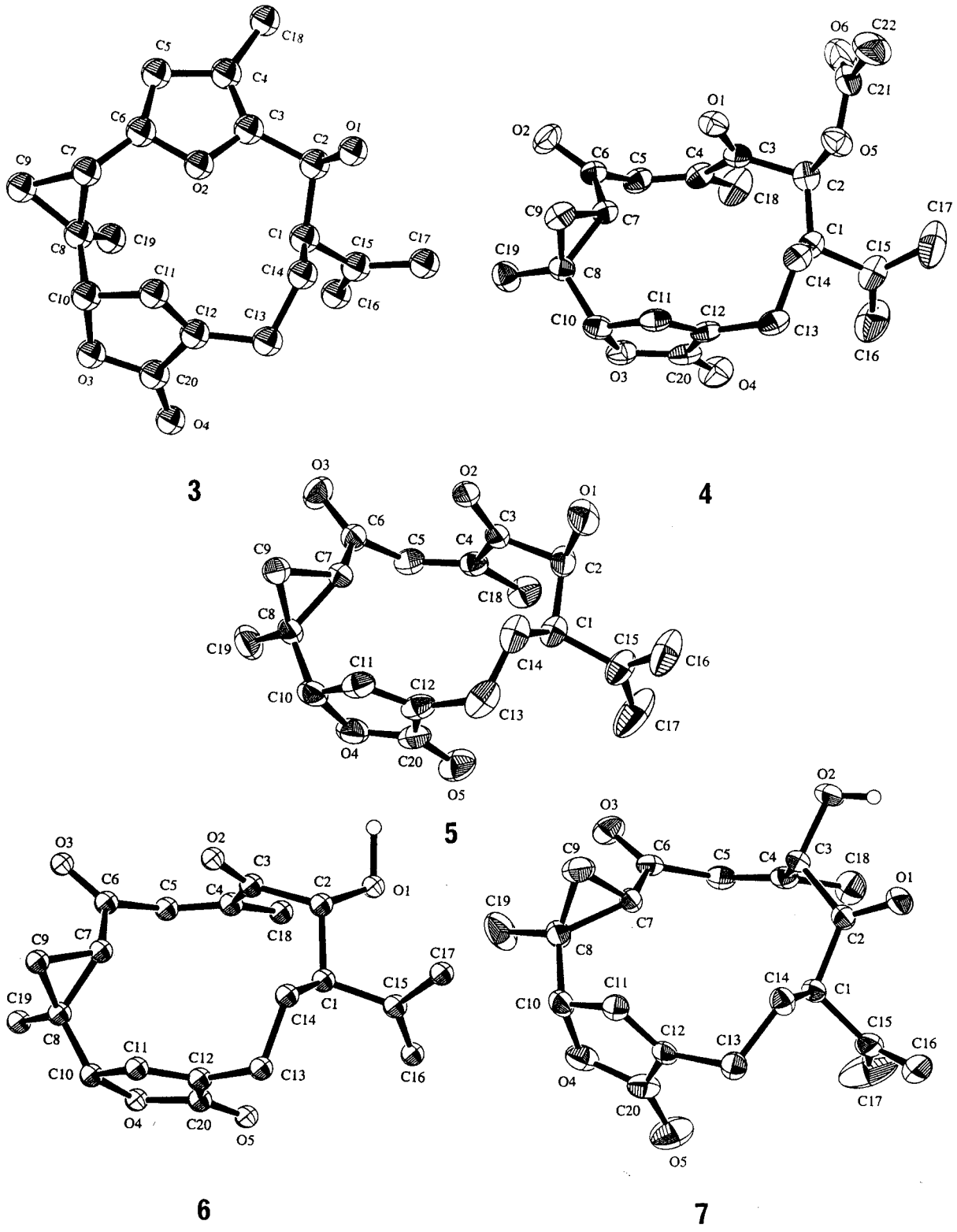

Figure 1. Computer-generated perspective drawings of the final X-ray crystallographic models of pinnatins A−E. Hydrogen atoms are omitted for clarity, and no absolute configuration is implied. The thermal ellipsoids are drawn at the 50% probability level. The drawings shown are the enantiomers of the structures drawn as **3**−**7**.

demonstrates unambiguously the biogenetic relationship between two diterpenoids of the cembrane and gersolane classes.

Results and Discussion

Isolation and Structure Elucidation. The gorgonian specimen was collected using SCUBA at a depth of 80−100 ft off San Andrés Island, Colombia, and was stored at −20 °C until extraction. The freeze-dried gorgonian (2.1 kg) was blended with MeOH−$CHCl_3$ (1:1), and after partitioning of the concentrated extract between hexane and H_2O, the aqueous suspension was extracted with $CHCl_3$. The $CHCl_3$ soluble fraction was chromatographed successively over silica gel and Bio-

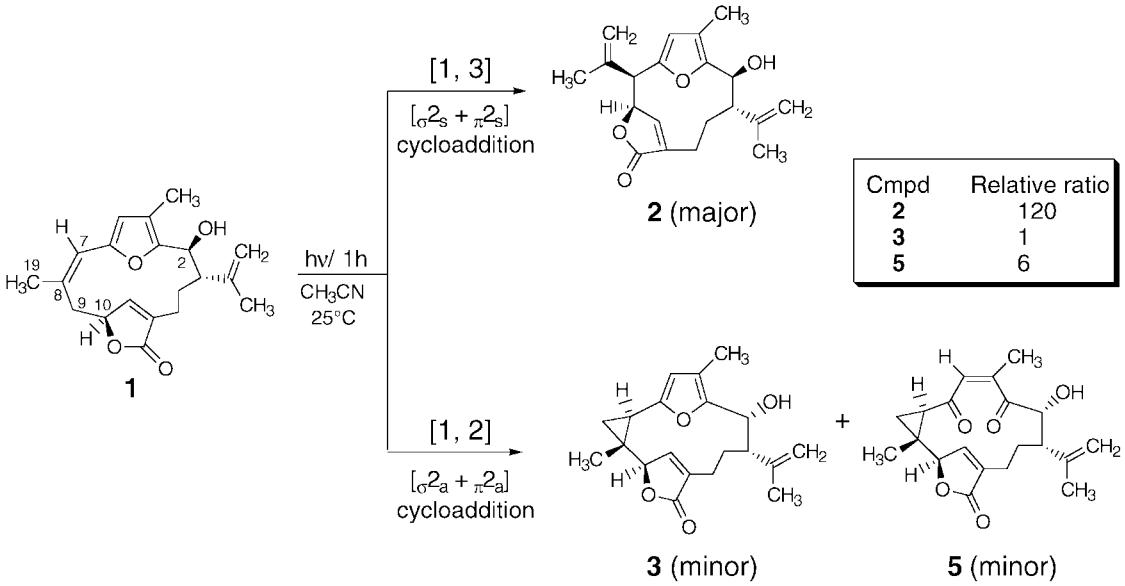

Figure 2. Cembrane−pseudopterane and cembrane−gersolane skeletal photoisomerizations are [$_{\sigma}2_s + _{\pi}2_s$] and [$_{\sigma}2_a + _{\pi}2_a$] cycloaddition processes, respectively, which are thermally forbidden but photochemically allowed. Upon irradiation, the C9−C10 σ bond of **1** migrates suprafacially to C7 with concomitant reorganization of the π system yielding **2** as the only [1,3]-allyl shift product. The configuration of the migrating α,β-unsaturated-γ-butenolide group remains unchanged during photoisomerization. Alternatively, the C9−C10 σ bond of **1** migrates antarafacially to C7 and C8, respectively, with retention of configuration at the migrating α,β-unsaturated-γ-butenolide group to yield **3** as a minor product. Although we are unable to detect it, inversion at the other end of the reacting σ bond (C-9 in **1**) is predicted. Under these reaction conditions, compound **3** is readily oxidized to afford pinnatin C (**5**) as the major [1,2]-allyl shift product. Curiously, only the cembrane−gersolane cycloisomerization process appears to be accompanied by a concurrent epimerization step at C-2.

Table 1. ^{1}H NMR (500 MHz) and ^{13}C NMR (125 MHz) Spectral Data of Pinnatins A−E in $CDCl_3$[a]

	pinnatin A (**3**)		pinnatin B (**4**)		pinnatin C (**5**)		pinnatin D (**6**)		pinnatin E (**7**)	
position	^{1}H mult (*J*)	^{13}C	^{1}H mult (*J*)	^{13}C	^{1}H mult (*J*)	^{13}C	^{1}H mult (*J*)	^{13}C	^{1}H mult (*J*)	^{13}C
1	2.15, br d (11.0)	50.6	2.55, br d (11.7)	42.0	2.50, br d (11.7)	45.2	2.87, m	46.4	3.44, br d (11.4)	51.4
2	4.63, br s	66.7	5.41, s	77.8	4.64, br d (6.3)	76.2	4.04, dd (10.6, 6.9)	78.3		208.1
3		150.2		197.3		203.6		206.9[b]	5.30, br s	75.2
4		116.9		140.4		139.3		139.2[b]		142.8
5	5.79, br s	109.1	6.03, q (1.5)	139.9	6.09, q (1.8)	140.4	6.00, q (1.5)	141.9[b]	6.07, br s	134.8
6		151.2		198.6		198.9		196.8[b]		197.8
7	1.79, dd (9.0, 7.2)	18.3	1.78, dd (8.4, 6.0)	28.3	1.73, dd (8.1, 6.0)	29.1	1.75, dd (8.6, 6.0)	30.9	2.17, dd (8.1, 6.0)	30.0
8		22.5		33.0		32.9		32.8		36.7
9α	1.42, dd (9.0, 6.0)	22.1	0.95, dd (8.4, 6.0)	16.8	0.94, dd (8.1, 6.0)	16.5	1.03, dd (8.6, 5.2)	18.2	1.24, dd (8.1, 5.1)	20.3
9β	1.31, dd (7.2, 6.0)		1.47, dd (6.0, 6.0)		1.46, dd (6.0, 6.0)		1.25, dd (6.0, 5.2)		1.56, dd (6.0, 5.1)	
10	4.81, br s	81.0	5.14, br s	83.4	5.15, br s	83.2	5.10, br s	83.2	5.24, br s	83.5
11	7.48, br d (1.5)	152.9	6.76, br d (0.6)	147.0	6.75, br s	146.6	6.66, br s	138.9	6.87, br s	146.4
12		130.6		139.9		140.5		144.0		138.8
13α	2.41, m	20.8	2.38, m	20.4	2.38, m	20.2	2.40, m	20.7	2.50, m	19.9
13β	2.39, m		2.35, m		2.34, m		2.35, m		2.42, m	
14α	2.50, m	26.1	2.14, m	29.7	2.05, m	29.7	2.34, m	29.7	1.48, m	33.4
14β	2.04, m		1.38, m		0.99, m		0.88, m		2.32, m	
15		146.2		143.1		144.7		142.7[b]		138.4
16α	4.83, m	112.8	5.06, m	115.8	5.04, m	115.6	5.19, m	115.8[b]	5.14, m	118.1
16β	4.72, br s		5.25, br s		5.27, br s		5.31, br s		4.94, br s	
Me17	1.85, br s	19.9	1.81, br s	19.5	1.89, br s	18.5	1.78, br s	18.2	1.87, br s	19.9
Me18	1.95, s	9.6	2.18, d (1.5)	20.6	2.09, d (1.5)	20.3	2.21, d (1.5)	21.6	1.63, d (3.6)	19.3
Me19	0.29, br s	13.6	1.26, br s	16.0	1.26, br s	16.1	1.53, s	15.7	1.49, s	15.2
20		174.9		173.6		173.5		173.8		172.5
21				170.1						
22			2.12, s	20.4						

[a] Assignments were aided by ^{1}H−^{1}H COSY, spin splitting patterns, comparison of *J* values, HMBC and HMQC experiments, numbers of attached protons as measured from DEPT spectra, and chemical shift values. The δ values are in ppm and are referenced to either the residual $CHCl_3$ signal (7.26 ppm) or $CDCl_3$ (77.0 ppm). [b]Due to intramolecular mobility at 25 °C this resonance line appeared as a broad, low intensity averaged signal. The precise location of the signal, therefore, is somewhat uncertain.

Beads SX-3, and fractions were monitored by TLC. While bipinnatin J (**1**) and kallolide A (**2**) were isolated as major products (combined yield 0.18% of dry weight), the pinnatins **3**−**7** were isolated as extremely minor components (combined yield 0.0012% of dry weight). Their molecular structures were established by extensive 1D and 2D NMR experiments (^{1}H−^{1}H COSY, long-range COSY, DEPT, NOESY, HMQC, and HMBC), IR, UV, and high-resolution EI mass spectral data. Crystallization of each pinnatin from EtOAc yielded colorless crystals suitable for X-ray studies. Detailed interpretation of these data permitted the assignment of all carbon and hydrogen atoms in pinnatins **3**−**7** unambiguously (see Table 1).

Pinnatin A (**3**), a minor and relatively unstable compound, mp 189−211 °C dec, $[\alpha]^{24}_D$ +225.4° (*c* 0.55, $CHCl_3$), $C_{20}H_{24}O_4$ by HREIMS, showed 20 resonances in its ^{13}C NMR spectrum which according to a DEPT spectrum were associated with three methyl, four methylene, six methine, and seven quaternary carbons. UV absorption at 216 nm, ^{13}C NMR signals at δ 151.2 (s, C-6), 150.2 (s, C-3), 116.9 (s, C-4), 109.1 (d, C-5), and 9.6 (q, C-18), a one-proton ^1H NMR singlet at δ 5.79, and a 3H singlet at δ 1.95, indicated that **3** possessed the same α,α'-disubstituted β-methylfuran constellation found in **1** and **2**. The ^{13}C NMR data further showed the presence of two double bonds (one was trisubstituted and the other 1,1-disubstituted) and one ester carbonyl (Table 1), thus requiring three carbocycles in addition to the furan ring. A series of NMR experiments enabled us to identify the α,γ-disubstituted-α,β-unsaturated-γ-lactone (δ 4.81, br s, 1H; 7.48, br d, 1H, J = 1.5 Hz) and isopropenyl (δ 4.83, m, 1H; 4.72, br s, 1H; 1.85, br s, 3H) residues in pinnatin A (**3**). A shielded quaternary carbon was observed at δ 22.5 (C-8), suggesting the presence of a cyclopropane ring. Information gleaned from COSY, NOESY, HMQC, and HMBC spectra (see Supporting Information) led to formulation of structure **3** for pinnatin A, and this was confirmed by X-ray crystallographic analysis.

A perspective ORTEP plot of **3** is shown in Figure 1. The X-ray experiment did not define the absolute configuration; the enantiomer drawn has been chosen arbitrarily to conform with the absolute configuration of kallolide A (**2**) at C-1.[9] This molecule contains an unprecedented 2,5-bridged furanogersolane carbocyclic skeleton which also features a hydroxyl group at C-2 in the α configuration. The overall conformation of the trans-fused bicyclo [11.1.0] carbon skeleton in the present structure has severely restricted rotation. Observation of an NOE between H-10/H-11, H-7/H-9α, H-7/H-11, and H-9β/Me-19 indicates that these proton pairs are on the same face of the molecule, and most importantly, the fact that no NOE was observed between Me-19 and protons H-7 or H-10 confirmed that the solution conformation is similar to that in the solid state as elucidated by X-ray analysis. Interestingly, while diterpenes **1** and **3** contain similarly functionalized chiral groups with identical relative stereochemistry (i.e., C-1 and C-10), the relative orientation of the C-2 hydroxyl group in pinnatin A (**3**) is clearly opposite to that found in the corresponding substructure of **1**. Pinnatin A (**3**) appears to be somewhat unstable. After several weeks inside an NMR tube in $CDCl_3$ at 25 °C, there was detectable decomposition to pinnatin C (**5**), another component isolated from the same $CHCl_3$ solubles (see below).

Pinnatin B (**4**), $[\alpha]^{24}_D$ −80.6° (*c* 0.90, $CHCl_3$), mp 212−249 °C dec, was assigned the molecular formula $C_{22}H_{26}O_6$ from mass spectral and ^{13}C NMR data, the latter consisting of 22 resolved signals corresponding to four methyl, four methylene, six methine, and eight quaternary carbons (DEPT). The HREIMS showed a molecular ion peak at *m*/*z* 386.1732. While the UV absorption maximum of **4** was similar to that of **3**, their molar absorptivities differed dramatically, 5300 in **4** vs 12800 in **3**. Six oxygens in the molecular formula were accounted for by two α,β-unsaturated ketones (carbonyl resonances at δ 198.6 and 197.3) and two esters (IR absorptions at 1749 and 1745 cm^{-1}, and ^{13}C resonances at δ 173.6 and 170.1), one of which was confidently ascribed to an acetate group [NMR signals at δ 2.12 (s, 3H); 170.1 (s) and 20.4 (q)]. The differences in structure between pinnatins A (**3**) and B (**4**) were traced to the furan and hydroxyl units in the former metabolite which appear modified in **4** as a methyl-substituted 3,6-dioxo-4-ene group (δ 6.03, q, 1H, J = 1.5 Hz; 2.18, d, 3H, J = 1.5 Hz) and an acetate (δ 2.12, s, 3H) unit, respectively. The structure of pinnatin B (**4**) assigned by spectral methods was confirmed by a single-crystal X-ray diffraction experiment which also yielded its relative stereochemistry. A perspective ORTEP drawing of pinnatin B is shown in Figure 1.

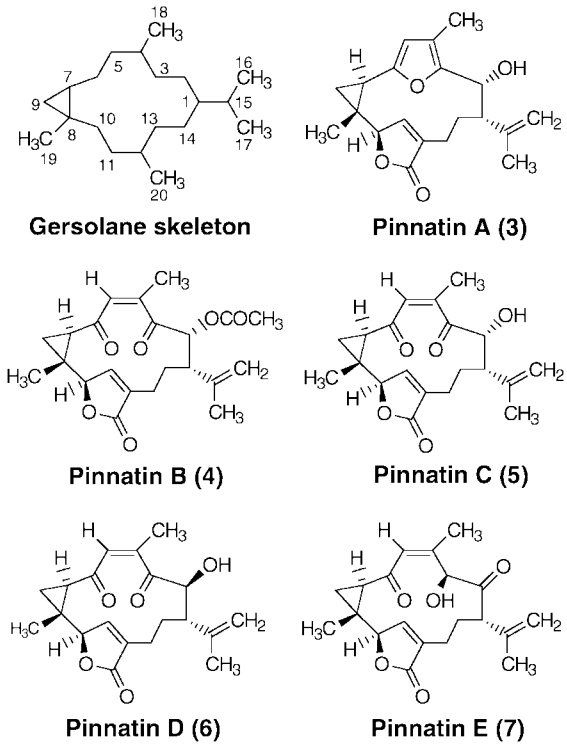

Pinnatin C (**5**) was obtained as colorless, platelet crystals, mp > 216 °C dec, $[\alpha]^{24}_D$ −140.0° (*c* 0.30, $CHCl_3$). The HREIMS of pinnatin C (**5**) exhibited its molecular ion at *m*/*z* 344.1629, appropriate for a molecular formula of $C_{20}H_{24}O_5$. The IR and UV spectra of **5** were similar to those of **4**. However, **5** showed a broad absorption at 3480 cm^{-1} that indicated the presence of a hydroxyl group. Except for the lack of signals ascribable to an acetate group, the ^1H and ^{13}C NMR data (Table 1) closely resembled those of **4**, and COSY, LR-COSY, HMQC, and HMBC spectra of **5** revealed that the two compounds have the same skeletal connectivities. Consequently, pinnatin C (**5**) was thought to be the deacetylated analogue of **4**. That the C-2 hydroxyl group appears located in the α-face of the molecule was evident from the NOE observed between H-2 and Me-18 in **5**. Thus pinnatin C was assigned structure **5**, and its structure was also confirmed by single-crystal X-ray diffraction (Figure 1). Since pinnatin C (**5**) could be produced from pinnatin A (**3**) by slow oxidation (as established by a series of TLC, HPLC, and ^1H NMR experiments), it may not be a true secondary metabolite. After several months of sitting at 25 °C in a $CDCl_3$ solution, compound **5** slowly began to decompose as revealed by periodic ^1H NMR and TLC tests.

(9) Marshall, J. A.; Bartley, G. S.; Wallace, E. M. *J. Org. Chem.* **1996**, *61*, 5729−5735.

Pinnatin D (**6**), the least abundant metabolite, was obtained as colorless needles, $[\alpha]^{24}_D$ +32.5° (*c* 0.40, $CHCl_3$), mp 213−220 °C, and decomposed quickly during melting point determination. The molecular formula $C_{20}H_{24}O_5$ was deduced from HREIMS and NMR data (Table 1) and was identical to that of pinnatin C (**5**), indicating that both compounds were isomers. Due to the small amount isolated, only weak ^{13}C NMR data were obtained for **6**, but interpretation of the COSY, LR-COSY, DEPT, and HMQC experiments and comparison of its NMR data with those of the other pinnatins led to the formulation of structure **6** for pinnatin D. Moreover, **6** gave rise to NMR spectra characterized by an abundance of broad signals of low intensity, suggesting rapid intramolecular mobility near the NMR probe temperature. Although HMBC data could not be obtained to provide evidence for connecting the smaller molecular segments deduced from vicinal couplings, long-range H−H couplings verified many of the connectivities between protonated carbons and quaternary centers. After the ^1H and ^{13}C data of **6** had been assigned by analysis of its 2D NMR spectra, it was obvious that the gross structure of pinnatin D (**6**) was the same as that of pinnatin C (**5**). Thus pinnatin D (**6**) was believed to differ from **5** only in relative stereochemistry at C-2. The relative configurations at chiral centers C-1, C-2, C-7, C-8, and C-10 were established by a single-crystal X-ray crystallography experiment (Figure 1). Interestingly, since the relative orientations around C-1, C-2, and C-10 in pinnatin D (**6**) are identical to those found in the corresponding similarly functionalized substructures of **1**, a close biogenetic relationship between these metabolites is implied.

Pinnatin E (**7**), mp 185 °C, $[\alpha]^{24}_D$ −290.0° (*c* 0.40, $CHCl_3$), a crystalline metabolite also having the formula $C_{20}H_{24}O_5$, was determined to be a functional group transposition isomer of **5** involving positions C-2,3 from detailed analysis of 1D and 2D NMR data which led to the assignments in Table 1. Most of the proton NMR spin systems were the same as those in the spectrum of **5**, and NOE's and long-range couplings supporting the connection of the various structural units were the same except for the methyl-substituted 3,6-dioxo-4-ene system. This compound exhibited ^1H and ^{13}C NMR spectra similar to those of **5** (see Table 1). Nevertheless, several major differences between **5** and **7** in the ^1H and ^{13}C NMR spectra were observed: the ^1H NMR signal ascribed to H-1 and Me-18 in **7** showed considerable differences in chemical shift and C-1 and C-3 had shifted from δ 45.2 and 203.6 in **5** to δ 51.4 and 75.2 in **7**, respectively. Functional group transposition of **7** at C-2 and C-3 would account for these spectral differences. The C-3 hydroxyl group must be located in the β-face of the molecule on the basis of a strong NOE observed between H-3 and H-7. The structure of **7** including its relative stereochemistry was confirmed by X-ray crystallography (Figure 1).

Biogenesis: Photochemical Interrelation of the Cembrane−Gersolane Skeletons. Insight into the biogenetic origin of the gersolane skeleton was gained by a closer examination of the photoproducts obtained upon photolysis of the conjugated furanocembrane bipinnatin J (**1**) (Figure 2). As mentioned in our earlier paper, irradiation of **1** in CH_3CN (quartz) for 2 h using a medium-pressure Xe (Hg) lamp yielded the pseudopterane kallolide A (**2**) as the sole photoisomer. At the end of this conversion, which was achieved in only 40% yield, we also recovered nearly 50% of unchanged **1**.[7] The configuration at the migrating α,β-unsaturated-γ-butenolide moiety remained unchanged during photoisomerization as predicted by the Woodward−Hoffmann rules of orbital symmetry for a suprafacial [1,3]-sigmatropic process. Alternatively, when a solution of analytically pure **1** in CH_3CN at 25 °C was irradiated for 1 h using a Pyrex vessel in place of quartz, again **2** was the major component of the reaction mixture (100% overall yield), but this time we detected the presence of two additional minor products by HPLC, namely, gersolanes pinnatin A (**3**) and pinnatin C (**5**). ^1H NMR and HPLC analyses of the unpurified material established the kallolide A (**2**)/pinnatin A (**3**)/pinnatin C (**5**) ratio as 120:1:6.[10] Since pinnatin C (**5**) must be produced by concurrent oxygenation of **3** (*vide supra*), kallolide A (**2**) and pinnatin A (**3**) are the only *de facto* photoisomers produced upon photolysis of **1**.[11] We were gratified to find that epimerization at C-2 of **1** took place completely during the cembrane−gersolane rearrangement.[12] The mechanism of the bipinnatin J (**1**) → pinnatin A (**3**) conversion is intriguing, and several possibilities may be considered. This striking propylene → cyclopropane cyclization accompanied by group migrations could well be a concerted transformation, although definite stereochemical information is lacking. Since pinnatin A (**3**) appears to be the sole photoisomer resulting from this novel cembrane−gersolane cycloisomerization process, this suggests that the photochemical interconversion did not involve a diradical mechanism but was instead consistent with a [1,2]-sigmatropic rearrangement.[13] Moreover, the configuration at the migrating stereogenic center remained unchanged during photoisomerization and, since no trace of other [1,2]-shift photoisomers was detected, the rearrangement must be intrinsically stereospecific.[14] Thus, our results suggest that the cembrane−gersolane rearrangement proceeds antarafacially with retention of configuration at the shifting α,β-unsaturated-γ-butenolide group and (presumably) inversion at the other end

(10) In our preliminary work we determined the ratio of lactones **2**, **3**, and **5** through integration of the vinylic CH_3 signals in the ^1H NMR spectrum of the mixture. Subsequent analysis by HPLC was in close agreement.

(11) Additional peaks were actually observed during HPLC analysis of the mixture. However, most of these spurious peaks turned out to be minor byproducts arising from concurrent photooxidation of kallolide A (**2**); see refs 7−9.

(12) We find it striking that irradiation with light in **1** leads to a [1,2]-allyl shift product displaying concurrent epimerization of the C-2 stereogenic center. Such a rather unpredictable result was not detected at the end of the [1,3]-allyl shift process. Though photochemical epimerizations usually imply that a radical intermediate might be involved in the course of the reaction, such an explanation would be inconsistent with the apparent high diastereoselectivity of the process. The difference in reactivity in **1** at C-2 during these sigmatropic rearrangements is unclear.

(13) The antarafacial [1,2]-sigmatropic shift with retention at one end and inversion at the other end of the reacting σ bond is also classified as a photochemically allowed $[{}_o2_a + {}_\pi2_a]$ cycloaddition reaction, see: Woodward, R. B.; Hoffmann, R. *The Conservation of Orbital Symmetry*; Verlag Chemie, Weinheim, and Academic Press: New York, 1970.

(14) For fundamental studies of photochemical [1,2]-allylic rearrangements; see (a) McCullough, J. J.; Manning, C. *J. Org. Chem*. **1978**, *43*, 2839−2842. (b) Akhtar, I. A.; McCullough, J. J.; Vaitekunas, S.; Faggiani, R.; Lock, C. J. L. *Can. J. Chem*. **1982**, *60*, 1657−1663.

(15) Addition of the σ bond is antarafacial if one terminus suffers inversion while the other suffers retention. In bipinnatin J (**1**), H-7 and Me-19 are cis. On the other hand, in pinnatin A (**3**) these groups end up being trans after the rearrangement. This is consistent with a mechanism in which the C9−C10 σ bond in **1** migrates antarafacially to C-7 and C-8, respectively, with inversion of configuration (undetectable) at one of the reaction termini and retention at the other (observed) to produce pinnatin A.

of the reacting σ bond.[15,16] Interestingly, while the di-π-methane reaction,[17] also a [1,2] sigmatropic rearrangement requiring 1,4-dienes or equivalent structures, is a very general and commonly observed photoreaction leading to vinyl cyclopropane rings, this is the first observation of this photochemical rearrangement in the production of natural products. Since there is no precedent for a photochemical one-carbon ring-contraction process leading to the formation of products such as pinnatin A (**3**), the cembrane−gersolane cycloisomerization reaction has important regio- and stereochemical implications. These results conclusively established the biogenetic interrelationship between the cembrane−gersolane skeletal systems.

Since the absolute configuration of kallolide A (**2**) has been established,[9] and both **2** and **3** have been correlated chemically with bipinnatin J (**1**), one can safely assume that they also have the same absolute configuration at all common chiral centers. The C-7,8,10 constellation in pinnatin A has been correlated with the C-1,2 array through their NOE's and by X-ray crystallographic analysis; therefore, the absolute configuration of chiral centers C-2, C-7, C-8, and C-10 must be as shown in structure **3**. Conceivably, the conversion in nature of **1** to isomers **2** and **3** could be an enzyme-mediated process. On the other hand, as long as gorgonians must inhabit areas exposed to sunlight for proper nutrition and growth, our results may suggest that such interconversions could also be induced by sunlight.

Biological Activity. Although the pinnatins A−E (**3**−**7**) were not isolated following a specific bioassay-guided separation protocol, follow-up biological screening indicated *in vitro* cytotoxic activity. The National Cancer Institute (NCI) *in vitro* primary disease-oriented antitumor screen was used to ascertain the cytotoxic properties of pinnatin A (**3**) and pinnatin B (**4**). Of the two compounds, pinnatin A (**3**) was the more potent, with concentrations of 10^{-5} M eliciting significant differential responses at the GI_{50} level from nearly all the renal, ovarian, colon, and leukemia cancer cell lines.[18] Pinnatin B (**4**) gave a similar pattern in the leukemia, melanoma, and breast tumor subpanels but required higher concentrations (10^{-4} M). Certain individual cell lines, however [e.g., NCI-H522 (lung cancer), HCT-116 (colon cancer), and MALME-3M (melanoma)], were substantially more sensitive than the average.

Experimental Section

General Experimental Procedures. Melting points were taken on a capillary apparatus and are reported uncorrected. Infrared spectra were recorded on a FT-IR spectrophotometer. ^{1}H and ^{13}C NMR spectral data and ^{1}H−^{1}H COSY, NOESY, HMQC, and HMBC experiments were measured on a 500 MHz FT NMR spectrometer. Column chromatography was performed on silica gel (35−75 mesh), and TLC analyses were carried out using glass silica gel plates. Normal-phase HPLC separations of natural products were performed on a Partisil 10 M9/50 silica gel with 15% 2-propanol in hexane. HPLC analysis of the irradiated solution of bipinnatin J (**1**) was performed on a Nucleosil Si (5 μm) column (250 × 4.6 mm) with 10% 2-propanol in hexane (flow rate, 0.50 mL/min; UV detector set at 218 nm). All solvents used were either spectral grade or were distilled from glass prior to use. Samples of **1** were photolyzed using a Xe (Hg) ozone-free 1000 W UV lamp with a 7-54 Corning filter connected to a lamp power supply. A water filter was used in front of the sample cell in order to minimize thermal degradation. The percentage yield of each compound is based on the weight of the dry gorgonian specimen.

Collection and Extraction of *Pseudopterogorgia bipinnata*. The Caribbean sea plume *P. bipinnata* was collected by hand using SCUBA at depths of 80−100 ft in May 1996 off San Andrés Island, Colombia. A voucher specimen is stored at the Chemistry Department of the University of Puerto Rico. The dry animal (2.1 kg) was blended with MeOH−$CHCl_3$ (1:1) (5 × 1 L), and after filtration, the crude extract was evaporated under vacuum to yield a green residue (167.5 g). After the crude extract was partitioned between hexane and H_2O, the aqueous suspension was extracted with $CHCl_3$ (4 × 1L). The resulting extract was concentrated *in vacuo* to yield 43.3 g of an oil which was chromatographed over silica gel (400 g) and separated into 30 fractions (I−XXX) on the basis of TLC analyses. Subsequent purification of fraction VIII (8.2 g) by column chromatography over silica gel (400 g) eluting with a gradient increasing EtOAc (0−100%) in hexane (100−0%) afforded 3.76 g of kallolide A (**2**) (0.18% yield) and 67 mg of bipinnatin J (**1**) (3.19×10^{-3}% yield). Fraction IX (0.89 g) was separated into three subfractions by size-exclusion chromatography on a Bio-Beads SX-3 column with toluene as eluent. The last fraction (0.26 g) was purified by HPLC [Partisil 10 M9/50 silica gel with 15% 2-propanol in hexane] to yield pinnatin A (**3**) (7.0 mg; 3.33×10^{-4}% yield), pinnatin B (**4**) (10.3 mg; 4.90×10^{-4}% yield), and pinnatin C (**5**) (3.4 mg; 1.62×10^{-4}% yield). Fraction X (1.09 g) was separated into four subfractions by size-exclusion chromatography on a Bio-Beads SX-3 column using toluene as eluent. The last fraction (0.45 g), which was purified by HPLC [Partisil 10 M9/50 silica gel with 15% 2-propanol in hexane], afforded pinnatin D (**6**) (0.8 mg; 3.81×10^{-5}% yield) and pinnatin E (**7**) (4.8 mg; 2.28×10^{-4}% yield).

Pinnatin A (3): colorless crystals; mp 189−211 °C dec; $[\alpha]^{24}_D$ +225.4° (*c* 0.55, $CHCl_3$); UV (MeOH) λ_{max} 216 nm (ϵ 12 800); IR (film) 3469, 2964, 1730, 1654, 1564, 1459, 1083, 1055, 988, 897, 888, 802 cm^{-1}; ^{1}H NMR ($CDCl_3$, 500 MHz) and ^{13}C NMR ($CDCl_3$, 125 MHz) (see Table 1); HREI-MS *m*/*z* [M$^+$] calcd for $C_{20}H_{24}O_4$ 328.1675, found 328.1673 (11), 310.1570 (5, $C_{20}H_{22}O_3$), 295.1333 (9, $C_{19}H_{19}O_3$), 242.0939 (12, $C_{15}H_{14}O_3$), 214.0989 (24, $C_{14}H_{14}O_2$), 213.0917 (26, $C_{14}H_{13}O_2$), 189.0914 (35, $C_{12}H_{13}O_2$), 163.0757 (95, $C_{10}H_{11}O_2$), 137.0601 (100, $C_8H_9O_2$), 124.0522 (44, $C_7H_8O_2$).

Single-Crystal X-ray Diffraction Analysis of Pinnatin A. Crystallization of pinnatin A by slow evaporation from EtOAc yielded colorless block crystals of excellent quality. A specimen of 0.37 × 0.31 × 0.24 mm was selected for the analysis. X-ray diffraction data were collected on a Siemens SMART CCD system at 23 ± 1 °C to a maximum 2θ of 54.2°, using Mo Kα radiation (λ = 0.71069 Å). Preliminary X-ray photographs showed orthorhombic symmetry and accurate lattice constants of a = 9.6790(6), b = 12.8769(9), and c = 14.328(1) Å. The systematic extinctions, crystal density (d_{calc} = 1.221 g/cm^3), and optical activity indicated space group $P2_12_12_1$ in the asymmetric unit (Z = 4) of composition $C_{20}H_{24}O_4$ with a formula weight of 328.41. Of the 9352 reflections measured, 2119 were unique (R_{int} = 0.023); equivalent reflections were merged. The crystallographic residual was R = 4.6% (R_w = 5.9%) for the observed reflections. The structure, which was solved by direct methods (SIR92) and completed

(16) Although antarafacial cycloaddition processes are impossible for transformations which occur within small or medium-sized rings, when the migrating group of atoms possesses an accessible π orbital and is not so substituted as to create an impossible steric situation in the transition state, alternative processes using that π orbital must be considered, and clearly, such changes must proceed with inversion at the migrating center. See: Woodward, R. B.; Hoffmann, R. *Angew. Chem., Int. Ed. Engl.* **1969**, *8*, 781−853.

(17) (a) Gilbert, A.; Baggott, J. *Essentials of Molecular Photochemistry*; Blackwell Scientific Publications: Oxford, 1991; pp 246−252. (b) Zimmerman, H. E. In *CRC Handbook of Organic Photochemistry and Photobiology*; Horspool, W. M., Song, P.-S., Eds.; CRC Press: Boca Raton, FL, 1994; pp 184−193.

(18) (a) Paull, K. D.; Shoemaker, R. H.; Hodes, L.; Monks, A.; Scudiero, D. A.; Rubenstein, L.; Plowman, J.; Boyd, M. R. *J. Natl. Cancer Inst.* **1989**, *81*, 1088−1092. (b) Boyd, M. R.; Paull, K. D. *Drug Dev. Res.* **1995**, *34*, 91−109.

by successive Fourier calculations, was refined by full-matrix least-squares methods, with anisotropic thermal parameters for all non-H atoms. Following initial refinement, H atoms were located from a difference Fourier map. HO8 was refined with a fixed isotropic thermal parameter, and all remaining H atoms were included in the final model at calculated positions, riding on the connected atoms. All calculations were performed with the teXsan crystallographic software package of Molecular Structure Corporation.[19] Neutral atom scattering factors were taken from *International Tables for X-ray Crystallography*.[20]

Pinnatin B (4): colorless crystals; mp 212−249 °C dec; $[\alpha]^{24}_D$ −80.6° (*c* 0.90, $CHCl_3$); UV (MeOH) λ_{max} 214 nm (ϵ 5300); IR (film) 3080, 2950, 1749, 1745, 1692, 1687, 1648, 1608, 1450, 1383, 1253, 1238, 1084, 977, 910, 893 cm^{-1}; ^1H NMR ($CDCl_3$, 500 MHz) and ^{13}C NMR ($CDCl_3$, 125 MHz) (see Table 1); HREI-MS *m*/*z* [M^+] calcd for $C_{22}H_{26}O_6$ 386.1729, found 386.1732 (3), 344.1620 (8, $C_{20}H_{24}O_5$), 326.1516 (7, $C_{20}H_{22}O_4$), 316.1660 (3, $C_{19}H_{24}O_4$), 298.1569 (8, $C_{19}H_{22}O_3$), 297.1492 (8, $C_{19}H_{21}O_3$), 255.1364 (3, $C_{17}H_{19}O_2$), 229.0867 (10, $C_{14}H_{13}O_3$), 221.1185 (52, $C_{13}H_{17}O_3$), 203.1071 (14, $C_{13}H_{15}O_2$), 193.1240 (14, $C_{12}H_{17}O_2$), 175.1124 (13, $C_{12}H_{15}O$), 151.0758 (18, $C_9H_{11}O_2$), 149.0605 (16, $C_9H_9O_2$), 139.0397 (22, $C_7H_7O_3$), 123.0452 (100, $C_7H_7O_2$), 105.0703 (13, C_8H_9), 79.0547 (19, C_6H_7).

Single-Crystal X-ray Diffraction Analysis of Pinnatin B. Crystallization of pinnatin B by slow evaporation from EtOAc yielded colorless needle crystals of excellent quality. A specimen of 0.31 × 0.16 × 0.13 mm was selected for the analysis. X-ray diffraction data were collected on a Siemens SMART CCD system at 23 ± 1 °C to a maximum 2θ of 54.0°, using Mo Kα radiation (λ = 0.710 70 Å). Preliminary X-ray photographs showed monoclinic symmetry and accurate lattice constants of a = 7.8795(8), b = 6.7101(6), and c = 19.764(2) Å. The systematic extinctions, crystal density (d_{calc} = 1.230 g/cm^3), and optical activity indicated space group $P2_1$ in the asymmetric unit (Z = 2) of composition $C_{22}H_{26}O_6$ with a formula weight of 386.44. Of the 5514 reflections measured, 2263 were unique (R_{int} = 0.000); equivalent reflections were merged. The crystallographic residual was R = 4.4% (R_w = 5.2%) for the observed reflections. The structure, which was solved by direct methods and completed by successive Fourier calculations, was refined by full-matrix least-squares methods, with anisotropic thermal parameters for all non-H atoms. Following initial refinement, H atoms were located from a difference Fourier map. HO8 was refined with a fixed isotropic thermal parameter, and all remaining H atoms were included in the final model at calculated positions, riding on the connected atoms. All calculations were performed with the teXsan crystallographic software package of Molecular Structure Corporation.[19] Neutral atom scattering factors were taken from *International Tables for X-ray Crystallography*.[20]

Pinnatin C (5): colorless crystals; mp 217−237 °C dec; $[\alpha]^{24}_D$ −140.0° (*c* 0.30, $CHCl_3$); UV (MeOH) λ_{max} 216 nm (ϵ 7800); IR (film) 3480, 3063, 2916, 1738, 1693, 1689, 1608, 1439, 1394, 1327, 1234, 1197, 1163, 1084, 972, 904 cm^{-1}; ^1H NMR ($CDCl_3$, 500 MHz) and ^{13}C NMR ($CDCl_3$, 125 MHz) (see Table 1); HREI-MS *m*/*z* [M^+] calcd for $C_{20}H_{24}O_5$ 344.1624, found 344.1629 (1), 326.1529 (1, $C_{20}H_{22}O_4$), 316.1667 (2, $C_{19}H_{24}O_4$), 315.1620 (6, $C_{19}H_{23}O_4$), 298.1572 (3, $C_{19}H_{22}O_3$), 297.1519 (9, $C_{19}H_{21}O_3$), 229.0874 (10, $C_{14}H_{13}O_3$), 221.1184 (16, $C_{13}H_{17}O_3$), 203.1083 (7, $C_{13}H_{15}O_2$), 193.1244 (10, $C_{12}H_{17}O_2$), 175.1122 (11, $C_{12}H_{15}O$), 151.0765 (15, $C_9H_{11}O_2$), 149.0609 (6, $C_9H_9O_2$), 139.0403 (20, $C_7H_7O_3$), 137.0609 (18, $C_8H_9O_2$), 123.0447 (100, $C_7H_7O_2$), 105.0705 (21, C_8H_9), 79.0553 (25, C_6H_7).

Single-Crystal X-ray Diffraction Analysis of Pinnatin C. Crystallization of pinnatin C by slow evaporation from EtOAc yielded colorless platelet crystals of excellent quality. A specimen of 0.21 × 0.17 × 0.06 mm was selected for the analysis. X-ray diffraction data were collected on a Siemens SMART CCD system at 23 ± 1 °C to a maximum 2θ of 54.1°, using Mo Kα radiation (λ = 0.710 69 Å). Preliminary X-ray photographs showed orthorhombic symmetry and accurate lattice constants of a = 32.885(2), b = 6.8859(4), and c = 7.9112(5) Å. The systematic extinctions, crystal density (d_{calc} = 1.277 g/cm^3), and optical activity indicated space group $P2_12_12_1$ in the asymmetric unit (Z = 4) of composition $C_{20}H_{24}O_5$ with a formula weight of 344.41. Of the 9516 reflections measured, 2177 were unique (R_{int} = 0.022); equivalent reflections were merged. The crystallographic residual was R = 5.3% (R_w = 7.3%) for the observed reflections. The structure, which was solved by direct methods (SIR92) and completed by successive Fourier calculations, was refined by full-matrix least-squares methods, with anisotropic thermal parameters for all non-H atoms. Following initial refinement, H atoms were located from a difference Fourier map. HO8 was refined with a fixed isotropic thermal parameter, and all remaining H atoms were included in the final model at calculated positions, riding on the connected atoms. All calculations were performed with the teXsan crystallographic software package of Molecular Structure Corporation.[19] Neutral atom scattering factors were taken from *International Tables for X-ray Crystallography*.[20]

Pinnatin D (6): colorless crystals; mp 213−220 °C dec; $[\alpha]^{24}_D$ +32.5° (*c* 0.40, $CHCl_3$); UV (MeOH) λ_{max} 210 nm (ϵ 12 200); IR (film) 3445, 3368, 3077, 2924, 1755, 1673, 1648, 1604, 1443, 1394, 1325, 1235, 1191, 1079, 1061, 975, 908, 893, 857, 807 cm^{-1}; ^1H NMR ($CDCl_3$, 500 MHz) and ^{13}C NMR ($CDCl_3$, 125 MHz) (see Table 1); HREI-MS *m*/*z* [$M-H_2O^+$] calcd for $C_{20}H_{22}O_4$ 326.1518, found 326.1510 (2), 298.1556 (1, $C_{19}H_{22}O_3$), 297.1479 (2, $C_{19}H_{21}O_3$), 229.0862 (7, $C_{14}H_{13}O_3$), 221.1172 (14, $C_{13}H_{17}O_3$), 203.1073 (6, $C_{13}H_{15}O_2$), 191.1067 (23, $C_{12}H_{15}O_2$), 175.1124 (11, $C_{12}H_{15}O$), 151.0755 (13, $C_9H_{11}O_2$), 149.0596 (5, $C_9H_9O_2$), 139.0393 (10, $C_7H_7O_3$), 137.0601 (15, $C_8H_9O_2$), 123.0443 (100, $C_7H_7O_2$), 111.0452 (27, $C_6H_7O_2$), 105.0705 (16, C_8H_9), 79.0541 (19, C_6H_7).

Single-Crystal X-ray Diffraction Analysis of Pinnatin D. Crystallization of pinnatin D by slow evaporation from EtOAc yielded colorless needle crystals of excellent quality. A specimen having approximate dimensions of 0.26 × 0.10 × 0.08 mm was mounted on a glass fiber. X-ray diffraction data were collected on a Siemens SMART CCD system at 23 ± 1 °C to a maximum 2θ of 54.2°, using Mo Kα radiation (λ = 0.710 70 Å). Preliminary X-ray photographs showed orthorhombic symmetry and accurate lattice constants of a = 6.7443(7), b = 15.899(2), and c = 16.906(2) Å. The systematic extinctions, crystal density (d_{calc} = 1.262 g/cm^3), and optical activity indicated space group $P2_12_12_1$ in the asymmetric unit (Z = 4) of composition $C_{20}H_{24}O_5$ with a formula weight of 344.41. Of the 9388 reflections measured, 2176 were unique (R_{int} = 0.001); equivalent reflections were merged. The crystallographic residual was R = 5.2% (R_w = 5.4%) for the observed reflections. The structure, which was solved by direct methods and completed by successive Fourier calculations, was refined by full-matrix least-squares methods, with anisotropic thermal parameters for all non-H atoms. Following initial refinement, H atoms were located from a difference Fourier map. HO8 was refined with a fixed isotropic thermal parameter, and all remaining H atoms were included in the final model at calculated positions, riding on the connected atoms. All calculations were performed with the teXsan crystallographic software package of Molecular Structure Corporation.[19] Neutral atom scattering factors were taken from *International Tables for X-ray Crystallography*.[20]

Pinnatin E (7): colorless crystals; mp 185 °C; $[\alpha]^{24}_D$ −290.0° (*c* 0.40, $CHCl_3$); UV (MeOH) λ_{max} 214 nm (ϵ 19 000); IR (film) 3394, 3090, 2950, 1760, 1719, 1667, 1657, 1202, 1067, 912, 871 cm^{-1}; ^1H NMR ($CDCl_3$, 500 MHz) and ^{13}C NMR ($CDCl_3$, 125 MHz) (see Table 1); HREI-MS *m*/*z* [M^+] calcd for $C_{20}H_{24}O_5$ 344.1624, found 344.1618 (1), 326.1514 (2, $C_{20}H_{22}O_4$), 316.1671 (2, $C_{19}H_{24}O_4$), 299.1630 (1, $C_{19}H_{23}O_3$), 298.1561 (1, $C_{19}H_{22}O_3$), 282.1608 (2, $C_{19}H_{22}O_2$), 229.1225 (3, $C_{15}H_{17}O_2$), 219.1023 (14, $C_{13}H_{15}O_3$), 203.1435 (8, $C_{14}H_{19}O$), 203.1069 (3, $C_{13}H_{15}O_2$), 191.1074 (31, $C_{12}H_{15}O_2$), 177.0911 (14, $C_{11}H_{13}O_2$),

(19) Molecular Structure Corporation (1985, 1992). *TEXSAN. Crystal Structure Analysis Package*. MSC, 3200 Research Forest Drive, The Woodlands, TX, 77381.

(20) Cromer, D. T.; Waber, J. T. *International Tables for X-ray Crystallography*, Vol. IV; The Kynoch Press: Birmingham, England, 1974; Tables 2.3.1 and 2.2A.

151.0757 (10, $C_9H_{11}O_2$), 135.0810 (9, $C_9H_{11}O$), 123.0445 (40, $C_7H_7O_2$), 111.0452 (100, $C_6H_7O_2$), 105.0706 (17, C_8H_9), 79.0544 (17, C_6H_7).

Single-Crystal X-ray Diffraction Analysis of Pinnatin E. Crystallization of pinnatin E by slow evaporation from EtOAc yielded colorless prism crystals, one of which having approximate dimensions of 0.23 × 0.19 × 0.17 mm was mounted on a glass fiber. X-ray diffraction data were collected on a Siemens SMART CCD system at 23 ± 1 °C to a maximum 2θ of 54.1°, using Mo Kα radiation (λ = 0.710 69 Å). Preliminary X-ray photographs showed orthorhombic symmetry and accurate lattice constants of a = 9.9170(5), b = 12.6694(7), and c = 14.4623(8) Å. The systematic extinctions, crystal density (d_{calc} = 1.259 g/cm^3), and optical activity indicated space group $P2_12_12_1$ in the asymmetric unit (Z = 4) of composition $C_{20}H_{24}O_5$ with a formula weight of 344.41. Of the 9640 reflections measured, 2164 were unique (R_{int} = 0.013); equivalent reflections were merged. The crystallographic residual was R = 4.1% (R_w = 4.7%) for the observed reflections. The structure, which was solved by direct methods (SIR92) and completed by successive Fourier calculations, was refined by full-matrix least-squares methods, with anisotropic thermal parameters for all non-H atoms. Following initial refinement, H atoms were located from a difference Fourier map. HO8 was refined with a fixed isotropic thermal parameter, and all remaining H atoms were included in the final model at calculated positions, riding on the connected atoms. All calculations were performed with the teXsan crystallographic software package of Molecular Structure Corporation.[19] Neutral atom scattering factors were taken from *International Tables for X-ray Crystallography*.[20]

Photolysis of Bipinnatin J (1). A solution of analytically pure bipinnatin J (5.2 mg) in acetonitrile (2 mL) was placed in a small Pyrex test tube and irradiated for 1 h. Analysis of the solution by TLC [silica gel UV_{254} precoated plates (0.25 mm) in 3% acetone in $CHCl_3$] and ^{1}H NMR spectroscopy revealed that the starting material **1** had disappeared and that the only major product obtained was identical to an authentic sample of kallolide A (**2**) [TLC retention time (R_f 0.41)]. After evaporation of the solution with N_2 followed by storage under high vacuum, a slightly yellow oily residue (6.5 mg, 100% crude yield) was obtained which was subsequently dissolved in dry acetonitrile (250 μL) and analyzed directly by HPLC. No trace of starting material bipinnatin J (**1**) was detected. In addition to kallolide A (**2**), which was the major component of the mixture, we tentatively identified two other minor components as pinnatin A (**3**) and pinnatin C (**5**) on the basis of their HPLC retention times. Retention times for standard solutions of authentic bipinnatin J (**1**), kallolide A (**2**), and pinnatins A (**3**), C (**5**), D (**6**), and E (**7**) in acetonitrile (3.0 mg/mL) after HPLC analysis in the same manner (min): bipinnatin J (13.3), kallolide A (14.1), pinnatin A (20.1), pinnatin C (26.5), pinnatin D (31.3), pinnatin E (29.2). Retention times (min) of HPLC peaks in the irradiated solution of bipinnatin J (**1**): 14.5 (kallolide A), 19.4 (pinnatin A), and 26.6 (pinnatin C).[11] The identity of each photoproduct (obtained in a ratio of 120:1:6, respectively) was subsequently confirmed by peak enhancement and ^{1}H NMR (500 MHz) experiments.[10]

Acknowledgment. This report is contribution No. 2 of the CMBN (Center for Molecular and Behavioral Neuroscience). The CMBN program is sponsored in part by National Institute of Health (NIH) Grant RO1 GM52277. We thank Mr. Javier J. Soto for the collection of *P. bipinnata* and Mr. Juan A. Sánchez for its taxonomic identification. We extend our sincere appreciation to V. L. Narayanan and Edward Sausville (National Cancer Institute) for cytotoxicity assays on human cells and to Dr. Rafael Arce (U.P.R.) for access to his photochemistry facilities. The HREIMS spectral determinations were performed by the Midwest Center for Mass Spectrometry, a NSF Regional Facility (Grant CHE8211164), and Mrs. Catherine Ramírez provided the 500 MHz HMBC spectra. Support for this research at U.P.R. was kindly provided by the NSF-EPSCoR (Grant R118610677), NIH-MBRS (Grant S06RR08102-17), and NSF-MRCE (Grant R11-8802961) programs.

Supporting Information Available: Description of the X-ray crystal structure data including large size ORTEP drawings, tables of intramolecular distances, torsion angles, positional parameters, and intramolecular bond angles for pinnatins A−E (**3**−**7**), the ^{1}H and ^{13}C NMR spectra and ^{1}H−^{1}H COSY, NOESY, and HMBC spectral data for compounds **3**−**5** and **7** (Tables S1−S4) (68 pages). This material is contained in libraries on microfiche, immediately follows this article in the microfilm version of the journal, and can be ordered from the ACS; see any current masthead page for ordering information.

JO980256B